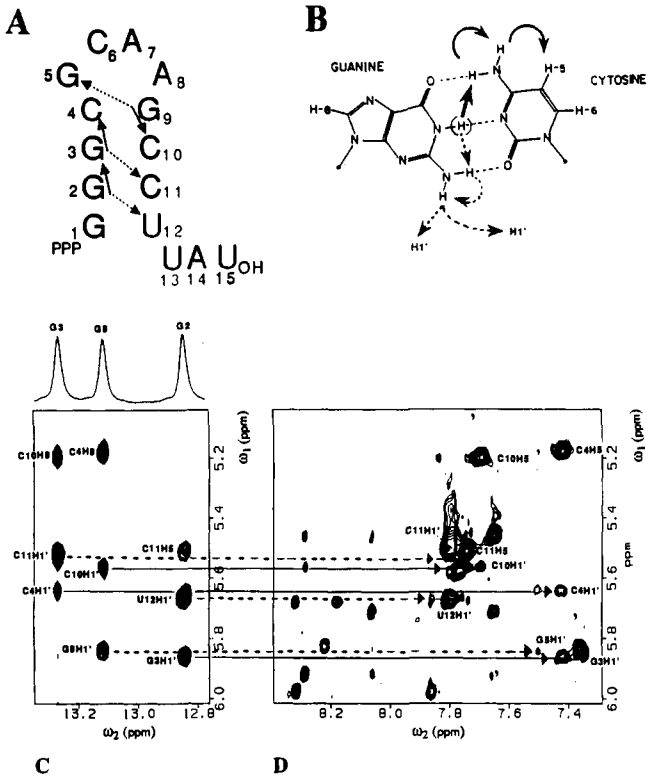

Figure 1. (A) Secondary structure model of the RNA hairpin. The hairpin contains four base pairs closed by a tetranucleotide loop and also has a trinucleotide 3′ dangling end. Arrows denote the intrastrand G imino proton to H1′ NOE connectivities (solid arrows) and the cross-strand G imino to H1′ NOE connectivities (dashed arrows) as discussed in the text. (B) Schematic of a GC base pair with the solid arrows showing the G imino–C amino–C5 proton connectivities and the dashed arrows showing the G–imino–G amino–C1′ proton connectivities used in resonance assignments. (C) Contour plot of a portion of the 2D NOE spectrum recorded in 90% H_2O at 5 °C showing part of the imino proton to the H1′/H5 region. The assigned imino proton region of the 1D NMR spectrum is shown on top of the contour plot. The spectrum was recorded by using a 1331 water suppression acquisition pulse[12] with 10K spectral width in both dimensions and a 400-ms mixing time. A homospoil pulse was applied in the mixing time to help eliminate residual transverse magnetization from the water protons. Ninety-six scans were taken with 4096 complex data points in the t_2 dimension and 300 complex FIDs in the t_1 dimension. The spectrum was apodized with a 65° shifted sine bell window function in both dimensions and zero-filled to 1K data points in t_1. In order to eliminate base-line roll caused by the 1331 water suppression pulse, a ninth degree polynomial base-line correction was applied to the imino proton region of the spectrum after Fourier transformation in t_2. (D) Contour plot of a portion of the 2D NOE spectrum recorded in D_2O at 5 °C showing the aromatic to H1′/H5 region. The arrows between parts C and D connect assigned cross peaks in D with cross peaks in C, with line styles corresponding to the arrows used in A. The spectrum was recorded with a 5K spectral width in both dimensions and a 400-ms mixing time. Ninety-six scans were taken in the t_2 dimension and 256 complex FIDs in t_1. The spectrum was apodized as in A, except that no base-line correction was performed.

system, and as observed for the RNA hairpin described above, every G imino proton in this region shows a set of three cross peaks to the H1′/H5 region. It is important to note that this cross peak pattern exists not only for the RNA helix II but also for helix I, which implies that this RNA–DNA helix also adopts an A-form type helix.

The cross peaks to the downfield-shifted C1′ protons, indicated by the arrows in Figure 2B, are extremely useful for resonance assignment in this system. These cross peaks arise from DNA C1′ protons, which tend to resonate more downfield than RNA C1′ protons and therefore now provide a number of specific starting points for the assignment of the proton resonances on the DNA strand. The resonance assignment for T9 H1′ was confirmed by the standard T methyl proton–H6–H1′ resonance pathway (unpublished results). The other imino proton–H1′ cross

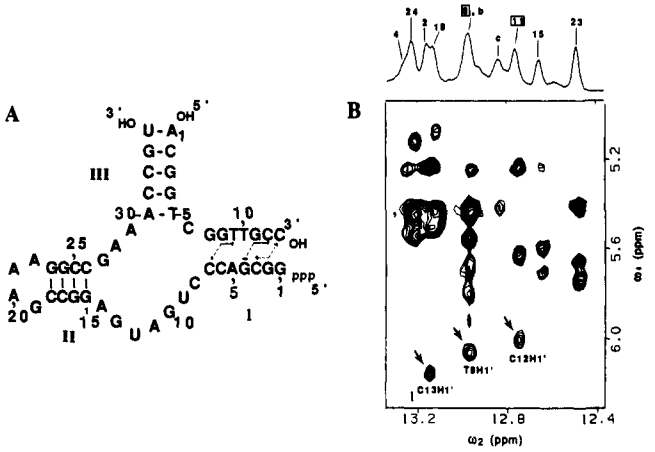

Figure 2. (A) Secondary structure model of a 34-mer hammerhead RNA enzyme base paired to a 13-mer DNA substrate. The RNA and DNA strands are numbered separately, and helices are defined by Roman numerals. Helix formation in II and III is indicated by solid lines between nucleotides (with these left out in helix I for clarity). For helix I, the G imino–C1′ proton connectivities discussed in the text are indicated by the solid or dashed arrows as defined in Figure 1. (B) The imino to aromatic proton region of the 2D NOE spectrum recorded at 15 °C of this RNA–DNA complex. Arrows indicate G imino–DNA C1′ cross peaks. The 1D NMR spectrum of this imino proton region is plotted above with the resonance assignments. Resonances involving imino protons on the DNA strand are boxed (letters indicate unassigned imino proton resonances[7]). The spectrum was recorded with a 200-ms mixing time with 128 scans in t_2 and 300 t_1 increments. Other data acquisition and apodization parameters were as described in the legend to Figure 1C.

peaks are being used as starting points for assignment of the rest of the DNA strand. The results presented here clearly show the usefulness of this novel resonance assignment procedure in RNA systems.

Acknowledgment. This work was supported by NIH AI 27026 and 30726, and the NMR spectrometer was purchased with partial support from NIH RR03283. We also thank the W. M. Keck Foundation for their generous support of RNA science on the Boulder campus.

Unprecedented Isomerization of an Aryl Nitrosyl Organometallic Complex to Its Arylimido Oxo Analogue[1]

Peter Legzdins,* Steven J. Rettig, Kevin J. Ross, and John E. Veltheer

Department of Chemistry
The University of British Columbia
Vancouver, British Columbia, Canada V6T 1Z1

Received November 20, 1990

Most transformations involving organometallic nitrosyl complexes result in the nitrosyl ligand remaining intact in the transition metal's coordination sphere.[2] A notable exception to this generalization involves the class of reactions summarized in eq 1 in which Cp′ = η^5-C_5H_5 (Cp) or η^5-C_5Me_5 (Cp*); M = Mo or W; R = alkyl[3a] or aryl.[3b] Reactions 1 thus result in the formal loss

$$Cp'M(NO)R_2 \xrightarrow[-{}^{\bullet}RNO^{\bullet}]{O_2} Cp'M(O)_2R \qquad (1)$$

of RNO upon treatment of the precursor complexes with molecular

(1) Organometallic Nitrosyl Chemistry. 46. Part 45: Dryden, N. H.; Legzdins, P.; Batchelor, R. J.; Einstein, F. W. B. *Organometallics*, in press.
(2) Richter-Addo, G. B.; Legzdins, P. *Chem. Rev.* **1988**, *88*, 991.
(3) (a) Legzdins, P.; Phillips, E. C.; Sánchez, L. *Organometallics* **1989**, *8*, 940 and references contained therein. (b) Legzdins, P.; Veltheer, J. E., manuscript in preparation.

0002-7863/91/1513-4361$02.50/0

Scheme I

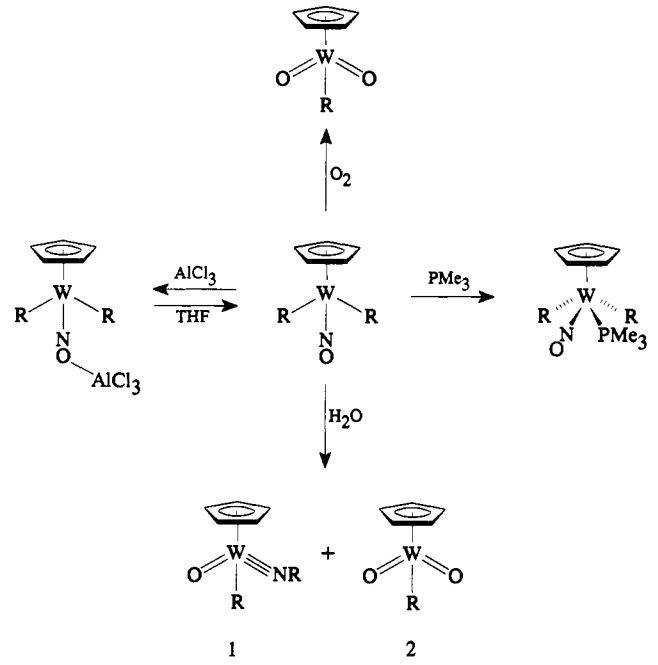

oxygen. We now report another type of transformation of a $Cp'M(NO)R_2$ complex which also affects the NO group, namely, the isomerization depicted in eq 2, which constitutes the first documented example of such a conversion. The other organo-

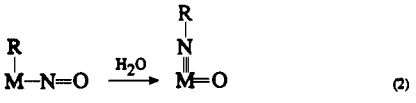

(2)

M = CpW(o-tolyl); R = (o-tolyl)

metallic product formed concomitantly during conversion 2 is the dioxo aryl complex, **2**, which is formed exclusively when the diaryl reactant is exposed to anhydrous O_2 (Scheme I).

In a typical experiment, a solid sample of purple $CpW(NO)(o\text{-tolyl})_2$[4] becomes a brown, oily solid when exposed to deaerated water vapor for 5 min at ambient temperatures. Soxhlet extraction of this solid with Et_2O affords yellow extracts which, when taken to dryness in vacuo, yield a yellow oil. Trituration of this oil with hexanes produces a yellow solid, which can be recrystallized from Et_2O to obtain analytically pure CpW(O)(N-*o*-tolyl)(*o*-tolyl) (**1**) as pale yellow plates (30% nonoptimized yield).[5] The product complex is a diamagnetic, air- and moisture-stable solid that is soluble in most common organic solvents.[6]

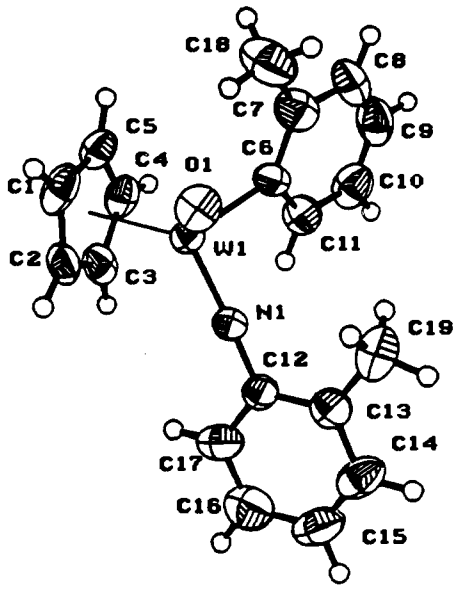

Figure 1. View of the molecular structure of CpW(O)(N-*o*-tolyl)(*o*-tolyl) (**1**). Selected bond lengths (Å) and angles (deg): W(1)–O(1) = 1.729 (4), W(1)–N(1) = 1.764 (5), W(1)–C(6) = 2.155 (6), W(1)–$Cp_{centroid}$ = 2.119 (3), N(1)–C(12) = 1.382 (8), O(1)–W(1)–N(1) = 106.8 (2), O(1)–W(1)–C(6) = 103.6 (2), N(1)–W(1)–C(6) = 95.0 (2), W(1)–N(1)–C(12) = 178.2 (5).

The solid-state molecular structure of **1** has been established by a single-crystal X-ray crystallographic analysis,[7] and an ORTEP plot of the structure is shown in Figure 1. The monomeric compound possesses a normal, three-legged piano-stool arrangement of ligands, the intramolecular dimensions of the CpW(O)(*o*-tolyl) fragment being comparable to those determined for related species. For instance, the tungsten–oxygen bond length in **1** (i.e., 1.729 (4) Å) resembles that found for $CpW(O)_2(CH_2SiMe_3)$ (i.e., average = 1.720 (5) Å),[8] and the tungsten–aryl carbon bond distance of 2.155 (6) Å is similar to the analogous bond length (average = 2.134 (8) Å) exhibited by $Cp^*W(NO)(o\text{-tolyl})_2$.[9] In other words, the intramolecular metrical parameters of **1** indicate that the aryl and oxo ligands function as one- and two-electron donors, respectively, to the tungsten center.[10] The most interesting features of the structure, however, involve the arylimido ligand, the relatively short W–N bond length (1.764 (5) Å) and the essentially linear W–N–C grouping (the angle at N being 178.2 (5)°) being consistent with the view that this ligand formally provides four electrons to the W≡N bond.[12] The spectroscopic properties of **1**[5] are also in accord with its retaining this molecular structure in solution. The transformation depicted in eq 2 thus results in the 16-valence-electron reactant complex being converted to its thermodynamically more stable 18-electron structural isomer.

The mechanistic details of conversion 2 are far from clear at present. In general, the characteristic chemistry of $CpW(NO)(o\text{-tolyl})_2$ (summarized in Scheme I)[13] resembles that established for other $Cp'M(NO)R_2$ complexes such as CpW-

(4) $CpW(NO)(o\text{-tolyl})_2$ was prepared by treatment of its dichloro precursor with 2 equiv of *o*-tolylmagnesium chloride in THF at −50 °C under an argon atmosphere. After being stirred for 1 h, the mixture was warmed to −10 °C, and the solvent was removed in vacuo. The thermally sensitive residue was suspended in 1:3 toluene/hexanes, and the resulting mixture was rapidly filtered at −30 °C through a column of Celite supported on a medium-porosity frit. Removal of solvent from the filtrate in vacuo afforded the desired bis(aryl) complex as a deep purple solid. IR (THF): ν_{NO} 1602 cm^{-1}. ^1H NMR (CD_2Cl_2): δ 7.56–7.02 (8 H, *o*-tolyl), 6.11 (s, 5 H, C_5H_5), 2.67 (s, 6 H, 2 × CH_3). Low-resolution mass spectrum (probe temperature 120 °C): *m/z* 461 (P^+).

(5) Anal. Calcd for $C_{19}H_{19}NOW$: C, 49.48; H, 4.15; N, 3.04. Found: C, 49.59; H, 4.30; N, 2.91. IR (Nujol mull): $\nu_{W=O}$ 897 (vs) cm^{-1}, also 1476 (s), 1379 (m), 1117 (m), 1022 (m), 1007 (m), 841 (m), 824 (s), 766 (s), and 750 (m) cm^{-1}. ^1H NMR (C_6D_6): δ 7.90 (dd, 1 H, *o*-tolyl), 7.24–6.77 (m, 7 H, *o*-tolyl), 5.72 (s, 5 H, C_5H_5), 2.48 (s, 3 H, CH_3), 2.32 (s, 3 H, CH_3). Low-resolution mass spectrum (probe temperature 120 °C): *m/z* 461 (P^+), 370 [P − (*o*-tolyl)$^+$].

(6) Product complex **2** is isolable by chromatography of the Et_2O-insoluble residue on alumina with acetone as eluant. IR (Nujol mull): $\nu_{W=O}$ 952 (s), 910 (s) cm^{-1}. ^1H NMR (C_6D_6): δ 7.80 (m, 1 H, *o*-tolyl), 7.12–6.98 (m, 3 H, *o*-tolyl), 5.68 (s, 5 H, C_5H_5), 2.27 (s, 3 H, CH_3). Low-resolution mass spectrum (probe temperature 120 °C): *m/z* 372 (P^+), 354 ($P - O^+$). The ratio of **1** to **2**, as determined by ^1H NMR spectroscopy of the final reaction mixture, is typically 1:2.

(7) Crystals of **1** are monoclinic of space group $P2_1/n$ (No. 14); a = 13.509 (3) Å, b = 7.003 (3) Å, c = 18.436 (3) Å, β = 107.24 (1)°; V = 1665.8 (7) Å^3; Z = 4; absorption coefficient = 70.82 cm^{-1}; diffractometer, Rigaku AFC6S; radiation, Mo Kα (λ = 0.710 69 Å); $2\theta_{max}$ = 60.1°; 2539 reflections with $I > 3\sigma(I)$; variable parameters = 199; R = 0.030, R_w = 0.029; goodness of fit indicator = 1.21. The non-hydrogen atoms were refined anisotropically, and hydrogen atoms were fixed in calculated positions with C–H = 0.98 Å.

(8) Legzdins, P.; Rettig, S. J.; Sánchez, L. *Organometallics* **1985**, *4*, 1470.

(9) Legzdins, P.; Rettig, S. J.; Veltheer, J. E., unpublished observations.

(10) According to the criteria developed by Parkin and Bercaw,[11] the $\nu_{W=O}$ of 897 cm^{-1} displayed by **1** in its Nujol mull IR spectrum indicates that the tungsten–oxygen linkage is principally a double bond.

(11) Parkin, G.; Bercaw, J. E. *J. Am. Chem. Soc.* **1989**, *111*, 391.

(12) Nugent, W. A.; Mayer, J. M. *Metal-Ligand Multiple Bonds*; Wiley-Interscience: Toronto, 1988; Chapter 5.

(13) Full details concerning the chemistry of $CpW(NO)(o\text{-tolyl})_2$ will be provided in a forthcoming full paper.

$(NO)(CH_2SiMe_3)_2$.[14] Thus, it forms simple 1:1 adducts with both typical Lewis acids and bases. The notable exception is its behavior upon treatment with water, the subject of this communication. Interestingly, if CpW(NO)(*o*-tolyl)$_2$ is treated with $^{18}OH_2$, the label is incorporated only into **2**. It thus appears that **1** and **2** are formed from CpW(NO)(*o*-tolyl)$_2$ via independent pathways. To date we have yet to find other experimental conditions for the conversion of CpW(NO)(*o*-tolyl)$_2$ to its isomer **1**.[15]

In addition to its unprecedented manner of formation via N–O bond cleavage, **1** is also the first cyclopentadienyl imido oxo complex to have been isolated.[16] It is analogous to the well-known dioxo and alkylidene oxo complexes, $CpW(O)_2R$ and CpW(O)(CHR')R, respectively.[3a] Furthermore, the availability of **1** also affords us, in principle, the opportunity to effect chemistry on a new chiral molecule containing two different types of multiple metal–ligand bonds. Studies directed toward this goal are currently in progress.

Acknowledgment. We are grateful to the Natural Sciences and Engineering Research Council of Canada for support of this work in the form of grants to P.L. and a graduate scholarship to K.J.R.

Supplementary Material Available: Tables of fractional coordinates and anisotropic thermal parameters for CpW(O)(N-*o*-tolyl)(*o*-tolyl) (**1**) (3 pages). Ordering information is given on any current masthead page.

(14) Legzdins, P.; Rettig, S. J.; Sánchez, L. *Organometallics* **1988**, *7*, 2394.
(15) CpW(NO)(*o*-tolyl)$_2$ does react with protonic acids and silver(I) salts, but these reactions do not produce complex **1**.[13]
(16) Ma, Y.; Demou, P.; Faller, J. W. *Inorg. Chem.* **1991**, *30*, 62.

Proton Exchange with Internal Water Molecules in the Protein BPTI in Aqueous Solution

Gottfried Otting, Edvards Liepinsh, and Kurt Wüthrich*

Institut für Molekularbiologie und Biophysik
Eidgenössische Technische Hochschule-Hönggerberg
CH-8093 Zürich, Switzerland

Received January 14, 1991

A high-resolution protein crystal structure usually includes the positions of numerous hydration water molecules. The Brookhaven protein data bank[2] thus includes the locations of over 30 000 water oxygen atoms. The large majority of these water sites form a hydration shell that covers large parts of the molecular surface. In addition, a smaller number of water molecules can be located in the interior of a protein and represent an integral part of the molecular architecture. Using high-resolution NMR[1] experiments we have started investigations of protein hydration in aqueous solution.[3] In 2D [^{1}H,^{1}H]-NOESY and 3D ^{15}N-correlated [^{1}H,^{1}H]-NOESY experiments and the corresponding measurements in the rotating frame, NOE cross peaks between protein protons and protons of interior water molecules could be identified in several small proteins.[3-5] In contrast, the NOEs expected to arise from close proximity of surface hydration waters to the protein were, as a rule, not observed. Similar observations were recently reported for interleukin 1β.[6] These data imply that the NOEs between protein protons and surface hydration water are quenched because the effective correlation time for positional rearrangement of the water protons relative to the protein surface, which is determined either by chemical exchange or by independent rotational motions of the water molecules, is much shorter than the rotational correlation time of the protein. For interior water molecules a *lower limit* of 0.3 ns for the lifetime of the protons with respect to exchange with the bulk water was derived from the fact that the observed NOEs have a negative sign.[3] In the present note we report new experiments with paramagnetic shift reagents, which provide an *upper limit* for this lifetime, and thus contribute a further fundamental detail toward a precise characterization of protein hydration in aqueous solution.

In all the aforementioned experiments[3-6] it was observed that the chemical shifts of interior water protons manifested in the NOE cross peaks with polypeptide protons are identical with that of the bulk water. This could be rationalized by two limiting situations: (i) The water chemical shifts in the protein interior and the bulk water are indeed identical. (ii) The interior water protons experience *conformation-dependent shifts* similar to those observed for the protons of polypeptide chains in globular proteins;[7] the presence of separate ^{1}H NMR signals for the interior water molecules would then have to be concealed by proton exchange or exchange of intact water molecules. Because it is not known whether there is indeed a chemical shift difference between interior hydration water and bulk water, a proper distinction between the limiting situations i and ii was so far not possible. In the experiment described in this note a defined chemical shift difference between bulk water and "inaccessible" interior water molecules was therefore established by addition of an extrinsic paramagnetic shift reagent.

In the protein BPTI four internal waters were previously identified in three different crystal structures[8] and by NMR in solution.[3] After addition of $CoCl_2$ to an aqueous solution of BPTI, the equilibria 1 and 2 are of interest in the present context. H*

$$Co^{2+}(H_2O)_6 + H^*{}_2O \underset{k_{-1}}{\overset{k_1}{\rightleftharpoons}} Co^{2+}(H_2O)_5(H^*{}_2O) + H_2O \qquad (1)$$

$$BPTI(H_2O)_4 + H'_2O \underset{k_{-m}}{\overset{k_m}{\rightleftharpoons}} BPTI(H_2O)_3(H'_2O) + H_2O \qquad (2)$$

and H' identify bulk water protons that are exchanged into binding sites of Co^{2+}, or interior sites in the protein, respectively. $H^*{}_2O$ and H'_2O are bound water molecules that contain one or two protons from the bulk water. The water molecules bound to Co^{2+} experience large chemical shifts and some broadening of the ^{1}H resonance lines due to the interactions with the unpaired electrons. It is known that the exchange k_1 is sufficiently fast for these paramagnetic effects to be averaged over the bulk water[9] and that a 30 mM concentration of Co^{2+} should cause a ^{1}H shift for the bulk water of approximately $\omega = 900\ s^{-1}$ at 600 MHz and 20 °C.[10]

Our measurements confirmed that the bulk water shift caused by addition of 30 mM $CoCl_2$ is approximately 0.25 ppm (arrows along ω_1 in Figure 1, parts A and B). Under these conditions a line broadening of 130 Hz for the bulk water is observed along ω_1 in Figure 1B, which is sufficiently small to allow observation of most of the previously identified NOEs between protons of the polypeptide chain of BPTI and the four interior water molecules (Figure 1B).[3] The NOESY cross peaks between different polypeptide protons of BPTI are virtually identical in parts A and B of Figure 1, which shows that the conformation of BPTI remained unchanged after addition of $CoCl_2$. The experiment of Figure

(1) Abbreviations used: NMR, nuclear magnetic resonance; 2D, two-dimensional; 3D, three-dimensional; NOESY, two-dimensional nuclear Overhauser enhancement spectroscopy; NOE, nuclear Overhauser enhancement; BPTI, basic pancreatic trypsin inhibitor.
(2) Bernstein, F. C.; Koetzle, T. F.; Williams, G. J. B.; Meyer, E. F., Jr.; Brice, M. D.; Rodgers, J. R.; Kennard, O.; Shimanouchi, T.; Tasumi, M. *J. Mol. Biol.* **1977**, *122*, 535-542.
(3) Otting, G.; Wüthrich, K. *J. Am. Chem. Soc.* **1989**, *111*, 1871-1875.
(4) Otting, G.; Wüthrich, K. In *Water and Ions in Biomolecular Systems*; Vasilescu, D., Jaz, J., Packer, L., Pullman, B., Eds.; Birkhäuser: Basel, 1990; pp 141-147.
(5) Wüthrich, K.; Otting, G. *Int. J. Quantum Chem.*, in press.
(6) Clore, G. M.; Bax, A.; Wingfield, P. T.; Gronenborn, A. *Biochemistry* **1990**, *29*, 5671-5676.
(7) Wüthrich, K. *NMR in Biological Research: Peptides and Proteins*; North-Holland: Amsterdam, 1976. Wüthrich, K. *NMR of Proteins and Nucleic Acids*; Wiley: New York, 1986.
(8) Deisenhofer, J.; Steigemann, W. *Acta Crystallogr.* **1975**, *B31*, 238-250. Wlodawer, A.; Walter, S.; Huber, R.; Sjölin, L. *J. Mol. Biol.* **1984**, *180*, 301-329. Wlodawer, A.; Nachman, J.; Gilliland, G. L.; Gallagher, W.; Woodward, C. *J. Mol. Biol.* **1987**, *198*, 469-480.
(9) Swift, T. J.; Connick, R. E. *J. Chem. Phys.* **1962**, *37*, 307-320.
(10) Luz, Z.; Shulman, R. G. *J. Chem. Phys.* **1965**, *43*, 3750-3756.

0002-7863/91/1513-4363$02.50/0